forests

MDPI

Article

Comprehensive Identification and Profiling of miRNAs Involved in Terpenoid Synthesis of *Gleditsia sinensis* Lam.

Yuzhang Yang [1,†], Jing Wang [1,†], Chun Wang [1], Hui Chen [1], Yanping Liu [2], Yanwei Wang [1,*] and Wei Gao [3,*]

[1] National Engineering Laboratory for Tree Breeding, Key Laboratory of Genetics and Breeding in Forest Trees and Ornamental Plants, Ministry of Education, The Tree and Ornamental Plant Breeding and Biotechnology Laboratory of National Forestry and Grassland Administration, College of Biological Sciences and Biotechnology, Beijing Forestry University, Beijing 100083, China; Yangyuzhang@bjfu.edu.cn (Y.Y.); Wangjing111@bjfu.edu.cn (J.W.); wangchun66@bjfu.edu.cn (C.W.); huichen@bjfu.edu.cn (H.C.)
[2] Henan Academy of Forestry, Zhengzhou 450008, China; lypbox@126.com
[3] College of Science, Beijing Forestry University, Beijing 100083, China
* Correspondence: ywwang@bjfu.edu.cn (Y.W.); w_gao@bjfu.edu.cn (W.G.); Tel.: +86-10-62336248 (Y.W.); +86-10-62338136 (W.G.)
† These authors contributed equally to this work.

Abstract: *Gleditsia sinensis* Lam. is a tree with worldwide distribution and important economic and medicinal values; its pods contain terpenoids including gleditsioside, thiamine, and brassinosteroids. However, thus far, there are few studies on the terpenoid regulation of *G. sinensis* at the molecular level. microRNA (miRNA) is a class of small RNAs with conserved and crucial roles in the regulation of diverse biological processes during plant growth and development. To identify the miRNAs of *G. sinensis* and evaluate their involvement in terpenoid synthesis, this investigation quantified the content changes in saponins in pods at three developmental stages: May (pod-setting stage), July (elongation stage), and September (browning stage), and then we performed genome-wide miRNA profiles during the three development stages of the *G. sinensis* pods. A total of 351 conserved miRNAs belonging to 216 families were identified, among which 36 conserved miRNAs exist specifically in legumes. Through target analysis, 708 unigenes were predicted to be candidate targets of 37 differentially expressed miRNAs. The targets of *miR838-3p* and *miR2093-5p* were involved in the derived branches of monoterpenes and gleditsioside, in brassinosteroid biosynthesis (BRB), and in indole alkaloid biosynthesis (IAB). Intriguingly, the targets of *miR829-3p.1* were predicted to take part in thiamine biosynthesis, and the targets of *miR4414b* and *miR5037a* were involved in the main process of cytokinin synthesis. The corresponding targets participated in BRB, IAB, and terpenoid backbone biosynthesis, which were enriched significantly, suggesting that *miR2093-5p*, *miR4414b*, *miR5037a*, *miR829-3p.1*, and *miR838-3p* play indispensable roles in the regulation of triterpenoid saponin and monoterpenoid biosynthesis. To date, this is the first report of miRNA identification in *G. sinensis* and miRNA expression profiles at different developmental stages of *G. sinensis* pods, which provides a basis for further uncovering the molecular regulation of terpenoid synthesis in *G. sinensis* and new insights into the role of miRNAs in legumes.

Keywords: *Gleditsia sinensis*; pods; miRNA; terpenoids; development

check for updates

Citation: Yang, Y.; Wang, J.; Wang, C.; Chen, H.; Liu, Y.; Wang, Y.; Gao, W. Comprehensive Identification and Profiling of miRNAs Involved in Terpenoid Synthesis of *Gleditsia sinensis* Lam. *Forests* **2022**, *13*, 108. https://doi.org/10.3390/f13010108

Academic Editors: Zhonghua Tang, Chao Wang and Fang Yu

Received: 26 November 2021
Accepted: 7 January 2022
Published: 12 January 2022

1. Introduction

Gleditsia sinensis Lam. belongs to *Leguminosae* sp., widely distributed throughout the world, especially in East and South Asia, and plays a crucial ecological role in soil and water conservation and landscaping. Moreover, the pods are extensively and increasingly used in medicine and detergent products [1]. In addition, the pods' terpenoids, including saponins, have important clinical effects in the treatment of diseases as part of traditional Chinese medicine in China.

To efficiently utilize the pods, the constituents of saponin, tannins, organic acid, alkaloid, axunge, and other terpenoids have been increasingly investigated [2]. Previous reports have shown that saponins are the main terpenoids of medicinal value of *G. sinensis* pods, and, thus far, there are more than 30 known saponins [3]. Moreover, the main bioactive substance occurring in a large proportion and with essential anti-tumor and anti-inflammatory roles in *G. sinensis* pods is gleditsioside, which is a kind of triterpenoid saponin [4–7].

Triterpenoid saponin consists of one pentacyclic sapogenin and several carbohydrate chains, and its main resource is isopentenyl diphosphate (IPP) produced from the mevalonate pathway (MVA) or the methylerythritol phosphate pathway (MEP) [8]. IPP, with its isomeride dimethylallyl diphosphate (DMAPP), is synthesized into geranyl diphosphate (GPP). Afterwards, IPP with GPP is further synthesized into farnesyl diphosphate (FPP). Then 2,3-oxidosqualene from two FPPs oxidized in sesquiterpenoid and triterpenoid biosynthesis (STTB) is cyclized for the pentacyclic skeleton by different oxidosqualene cyclases (OSCs) [9]. The pentacyclic skeleton is finally decorated with hydroxy by cytochrome P450 monooxygenases (P450s) and carbohydrate chains catalyzed by UDP-dependent glycosyltransferases (UGTs) to form triterpenoid saponins [10]. Moreover, 2,3-oxidosqualene is not only the precursor of saponin, but also the precursor of sterols from steroid biosynthesis (STB) and its derivative in brassinosteroid biosynthesis (BRB) [11]. Moreover, many intermediates during triterpenoid saponin biosynthesis are also important precursors of other terpenoids. For example, DMAPP and GPP are the only resource of cytokinins in the zeatin pathway (ZTB) [12] and monoterpenoids in monoterpenoid biosynthesis (MTB), respectively. However, unlike all primary metabolites, some terpenoids become necessary and beneficial for plant growth only when they reach a certain concentration, which is regulated by unique mechanisms in plants [13]. Among these mechanisms, regulation mediated by microRNA (miRNA) is especially important. Recently, several miRNAs involved in the STTB pathway have been mapped and validated in *X. strumarium* L. using NGS technology. For example, mRNAs encoding the upstream enzymes in the pathways of terpenoid biosynthesis, including IPP and DMAPP, were predicted to be targeted by *miR7539*, *miR5021*, and *miR1134* [14]. Moreover, a review further summarized the critical roles of the miRNA–mRNA module in terpenoid biosynthesis and accumulation, which opens a new perspective for further investigations [15].

The miRNA is a kind of single-strand, small non-coding RNA with a length of 21–24 nt and can regulate the development and stress responses of plants, such as disease resistance [16], flower blooming regulation [17], and the promotion of pod ripening [18,19], by preventing mRNA translation or mRNA cleavage at the post-transcription level. Interestingly, previous investigations have shown that miRNAs participate in the secondary metabolite synthesis pathway, and the contents of some metabolites are co-regulated by multiple miRNAs in plants. For example, in *Arabidopsis thaliana* (L.) Heynh., the expression of *MYBL2* was suppressed by both *miR858a* and *HY5* (elongated hypocotyl 5), which leads to activation of anthocyanin synthesis pathways [20]. In addition, *miR9662*, *miR894*, *miR172*, and *miR166* were suggested to regulate saponin biosynthesis in *Chlorophytum borivilianum* Santapau & R.R.Fern. [21], which indicated that miRNAs are key molecular determinants in the saponin biosynthesis pathway.

However, thus far, there are few reports of miRNAs in *G. sinensis*, especially miRNAs involved in the regulation of gleditsioside synthesis, which varies with the development in *G. sinensis* pods. Consequently, it is indispensable to investigate the involvement of miRNAs in triterpenoid saponin synthesis in *G. sinensis*. In this investigation, the conserved and special miRNAs were first identified among three different stages of pods (May, July, and September). Thereafter, the expression profiles of the miRNAs from the three stages with different quantities of gleditsioside were compared. Based on this, the targets of miRNAs with differential expression patterns were further predicted, and the function was annotated. As a result, a total of 351 conserved miRNAs belonging to 216 families were identified, among which 36 conserved miRNAs exist specifically in legumes. Furthermore,

67 novel miRNA candidates were identified. Intriguingly, *miR2093-5p*, *miR4414b*, *miR5037a*, *miR829-3p.1*, and *miR838-3p* were shown to be involved in the regulation of triterpenoid saponin and MTB biosynthesis. The targets of *miR838-3p* and *miR2093-5p* were downregulated with the development of the pods and are suggested to be involved in the derived monoterpenes and gleditsioside branches in the BRB and IAB synthesis pathway. Whereas the targets of *miR4414b* and *miR5037a* were showed to be involved in the main pathway of cytokinin synthesis. The differential expression and target prediction showed that *miR9736*, *miR2658*, *miR396b*, and *miR156d-3p* might play a role in the development of *G. sinensis* pods. Taken together, this investigation should clarify the molecular regulation mechanism of terpenoids, especially saponin synthesis and important candidate genes, for further promotion of triterpenoid saponin production in *G. sinensis* pods at the molecular level.

2. Materials and Methods

2.1. Material Collection and Determination of Saponin Contents

G. sinensis pods were sampled with the seeds excluded at the setting stage (May), elongation stage (July), and browning stage (September), respectively, in Beijing Forestry University (40°0′18″ N, 116°20′13″ E). Pooled sampling was performed with five mixed pods at the same site of the *G. sinensis* tree and collected each month with three biological replicates. The samples were immediately frozen in liquid nitrogen and stored at −80 °C. The pods and leaves were ground under liquid nitrogen, and 3 g of the sample powder was put into a 50 mL centrifuge tube; this was repeated three times, followed by the addition of 30 mL anhydrous ethanol, soaked evenly, and then the samples were put into an ultrasonic cleaner for 1 h, respectively, and left for 20 min. After filtration, the samples were diluted with anhydrous methanol and mixed evenly. The standard curve method was used for the color reaction. A total of 1 mg/mL echinocystic acid (EA) from Shanghai Yuanye Biological Co., Ltd. (Shanghai, China), was used as a standard compound, diluted with anhydrous methanol into 20 μg/mL, 40 μg/mL, 60 μg/mL, 120 μg/mL, 160 μg/mL, and 200 μg/mL tested solutions, respectively, for the color reaction. A UV absorption spectrometer was used for full wavelength scanning at 400–700 nm to determine the highest absorption peak of each sample. The content of gleditsioside (%) = $\alpha \times (V1/V2) \times (N/M)$, ($\alpha$: absorbency of methanol solution after color reaction at 538 nm; V1: initial volume of gleditsioside extract; V2: volume of the sample for color reaction; N: dilution multiple of gleditsioside extract; and M: powder of pods for extraction).

2.2. RNA Extraction

Total RNA was extracted from the pods of GSM (May), GSJ (July), and GSS (September) with two replicates for each period as described previously [22] with an improved RNA procedure by our lab [23]. The concentration and purity were detected by a Nano Photometer® spectrophotometer (Implen, Westlake Village, CA, USA).

2.3. Library Preparation and Sequencing

Small RNA (sRNA) libraries were constructed as described previously [24]. Briefly, small RNA (sRNA) with a size of 18–30 nt was isolated, and then a Pre-Kit was used to ligate the 5′ adaptor and 3′ adaptor of the RNA, followed by reverse transcription and then PCR (polymerase chain reaction) amplification. The sRNA was sequenced by an Illumina Hiseq 2500 sequencing system from the 1 GENE company (Hangzhou, China).

2.4. Sequence Filtration and sRNA Clustering

The raw data were first processed to remove low-quality reads and contaminants, including sequences with a poly N or 5′ adaptor, without a 3′ adaptor insert tag, and containing poly A/T. Thereafter, clean reads were obtained. To classify the sRNA comprehensively, clean reads were further aligned to the repeat sequence and the GenBank (https://www.ncbi.nlm.nih.gov/, accessed on 19 March 2021), Rfam (http://rfam.xfam.org/, accessed on 21 March 2021), and miRBase (http://www.mirbase.org/, accessed on

26 March 2021) databases. Through the alignment with GenBank and Rfam, rRNA, scRNA, snoRNA, snRNA, and tRNA were excluded from the clean reads. Additionally, sRNAs derived from the exon and intron of the mRNA were also discarded. To obtain a unique annotation for each sRNA, the following criterion was applied: rRNA > conserved miRNA > repeat > exon > intron, with a preference for GenBank annotation over that of Rfam.

2.5. Identification of Conserved and Novel miRNAs

MiRNAs were identified using unigenes of *G. sinensis* as the reference. sRNAs that were matched to miRBase (version 22.0) (http://mirbase.org/index.shtml, accessed on 9 April 2021) and had no more than five mismatches were classified as known miRNAs of *G. sinensis*. UNAFold (http://www.unafold.org/mfold/applications/rna-folding-form.php, accessed on 15 April 2021) and Mireap (http://sourceforge.net/projects/mireap/, accessed on 18 April 2021) were used to predict the precursors of novel miRNAs as described previously [25].

2.6. Differential Expression Analysis of miRNA and Functional Annotation of Target Genes

Read counts of each unique miRNA were normalized by DESeq for differential analysis. miRNAs with averaged reads of less than 10 in all 3 periods were excluded for differential expression analysis. miRNAs with a fold change of $|\log2\ (\text{ratio})| \geq 1$ and a p-value of <0.05 were regarded as differentially expressed.

2.7. Target Prediction and Functional Annotation

The target prediction of miRNAs with differential expression was conducted as previously described [26] using unigenes of *G. sinensis* as a reference. Using the program's default parameters, the target genes were predicted by psRNATarget (http://plantgrn.noble.org/psRNATarget/, accessed on 18 May 2021) [27]. For the KEGG or GO annotation of the targets, an enrichment analysis was performed and the p-value and the corrected p-value (q-value) of the hypergeometric test were calculated [28]. KEGG pathways or GO terms with a p-value or q-value of no more than 0.05 were defined as significantly enriched.

3. Results

3.1. Accumulation of Saponins in G. sinensis Pods with Different Developmental Stages

Based on the field observations, the pods were formed in the beginning of May when seed formation was not visible (Figure 1a). As the pods continued to develop until July (Figure 1b), the whole pods expanded fully, the width of the pods no longer changed, and green seeds were visible and could be peeled out. By September (Figure 1c), the pods started to turn yellow, and, interestingly, a strong pungent odor was detected during the process of seed stripping, implying that there might be more abundant saponins produced in September.

To detect the changes in gleditsioside accumulation with the development of *G. sinensis* pods, the concentration of saponins in the three stages was quantified by spectrophotometry colorimetry with echinocystic acid (EA). We found that only the maximum absorption wavelength of the methanol extraction of *G. sinensis* pods was similar to that of EA, and it was much closer to 538 nm (Figure S1a), and the absorbance of the EA solution was proportional to its weight (Figure S1b), suggesting that we could regard EA as the standard by which to quantify gleditsioside content.

As a control, the leaves contained a much smaller amount of saponins (2.2%) (Table S1). Intriguingly, the saponin content of the pods showed a trend of increasing gradually with the development stages of the *G. sinensis* pods. The OD values showed a trend of monthly accumulation, which was increased significantly in September (Figure 2), and the contents of saponins were 9.3%, 9.4%, and 10.6% in the pods at the setting stage, elongation stage, and browning stage, respectively.

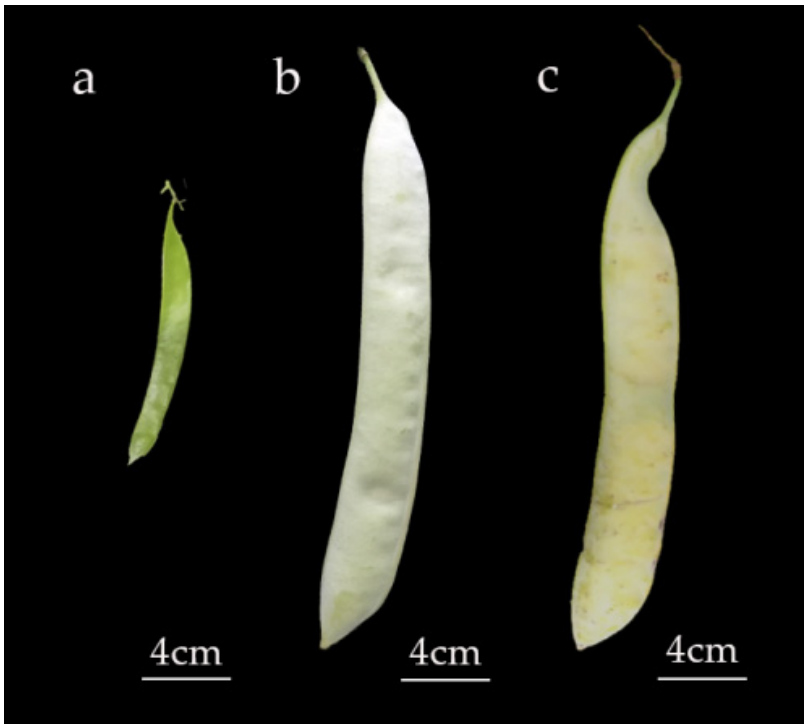

Figure 1. *Gleditsia sinensis* pods at the fruit-setting stage (**a**), elongation stage, (**b**) and browning stage (**c**).

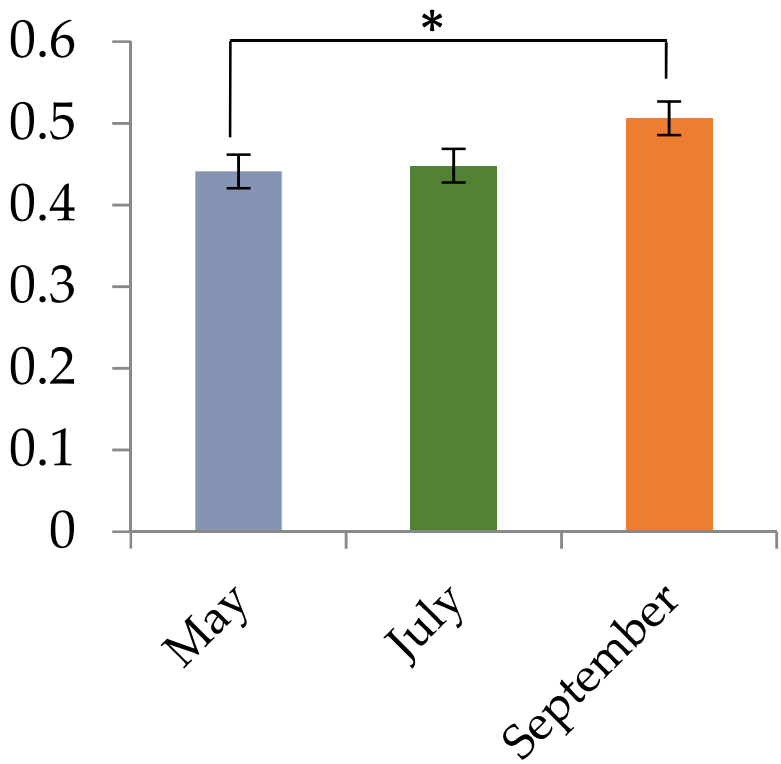

Figure 2. Absorbance of *Gleditsia sinensis* pod extract in May, July, and September. Note: The ordinate represents absorbance after colorimetry of the pod extract at three stages. (*): p-value ≤ 0.05, significant difference.

3.2. Small RNA Sequencing of G. sinensis Pods at Three Different Developmental Stages

Based on the accumulation of saponins in *G. sinensis*, we further conducted sRNA sequencing for pods at different developmental stages: GSM (May), GSJ (July), and GSS (September). A total of 11,148,921 (GSM), 13,875,552 (GSJ), and 13,289,369 (GSS) clean reads were obtained; among these reads, 2,917,967 (GSM), 1,362,408 (GSJ), and 1,728,910 (GSS) reads were unique according to alignment with the Rfam and Repbase databases. These reads were classified into miRNA, rRNA, Repeat, snRNA, snoRNA, tRNA, and Unann (Table 1). The distribution of sRNA with different lengths from *G. sinensis* pods was analyzed. We found that 21–24 nt sRNAs accounted for the largest proportion of total RNA in each sample (Figure 3), which is consistent with the typical distribution of sRNAs for Dicer-derived products and is similar to previous reports regarding trees [29,30].

Table 1. Analysis of small RNA sequences from the libraries of *Gleditsia sinensis* pods at different developmental stages.

Sample	Class	miRNA	rRNA	Repeats	snRNA	snoRNA	tRNA	Unann	
GSM	Unique	48,994	451,446	23	9514	9217	18,152	2,380,624	2,917,967
	Total	1,036,235	4,235,848	27	58,957	57,321	209,420	5,551,115	11,148,921
GSJ	Unique	50,507	636,727	1	6479	4269	5706	658,720	1,362,408
	Total	1,078,946	10,808,395	1	144,310	19,019	36,019	1,788,863	13,875,552
GSS	Unique	49,288	597,554	14	5336	5117	26,131	1,045,473	1,728,910
	Total	976,674	8,687,031	19	95,666	35,275	251,696	3,243,009	13,289,369

Note: miRNA, microRNA; rRNA, ribosomal ribonucleic acid; Repeat, repeat sequence; snRNA, small nuclear ribonucleic acid; tRNA, transfer RNA; Unann, unannotated reads.

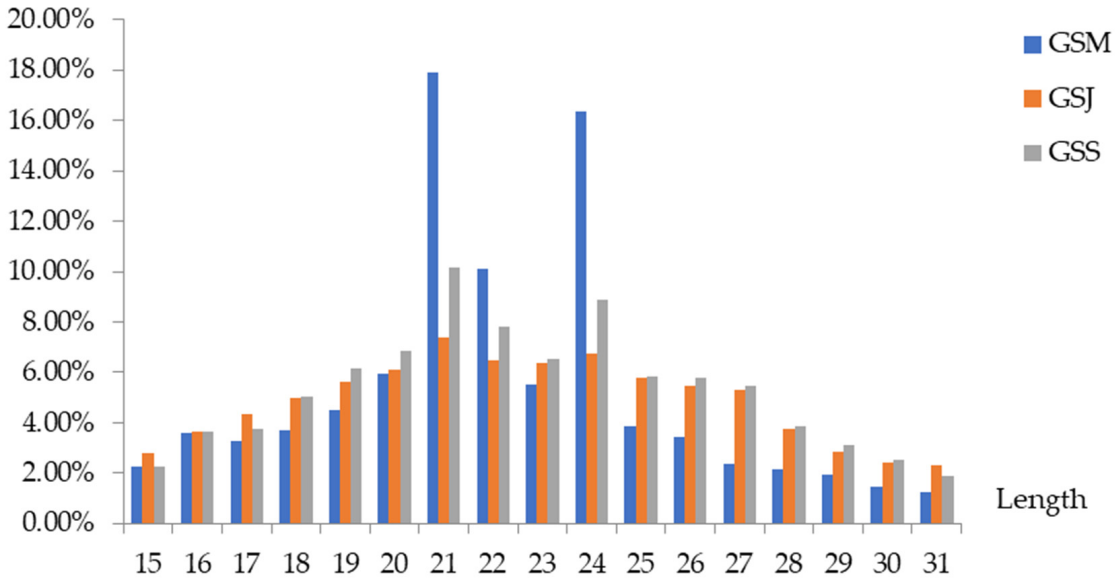

Figure 3. Differential expression levels of sRNA with different lengths in *Gleditsia sinensis* pods. Note: May (GSM), July (GSJ), and September (GSS); *X*-axis represents the length of miRNA, and the *Y*-axis represents the proportion of sRNAs of different lengths to total RNA. The statistics of the length distribution were based on unique valid reads.

3.3. Identification of Conserved miRNAs in G. sinensis Pods

Through the alignment with the miRBase, 351 conserved miRNAs belonging to 216 families were found (Tables S2 and S3). Among them, 214 known miRNAs in 153 families were in GSM, 118 known miRNAs in 71 families were in GSJ, and 235 known miRNAs in 142 families were in GSS, respectively. Interestingly, 71 miRNAs were detected to be expressed in all developmental stages (Table S2). Furthermore, more than 95 miRNAs only existed in GSM or GSS. For example, *miR396b-5p* was only detected in GSM with high

abundance, and *miR2095-3p* was only detected in GSS, while *miR396b* and *miR8682* were only detected in GSS (Table 2).

Intriguingly, in this investigation, we discovered that 36 conserved miRNAs exist only in legumes (Table 3), which further provides molecular proof that *G. sinensis* should be classified as Leguminosae sp.

Table 2. Highly expressed conserved miRNAs in *G. sinensis* pods with different developmental stages.

miRNA	Read Count			Sequence (5′-3′)
	GSM	GSJ	GSS	
miR7984a	82,492.5	268,297.5	208,928.5	UCCGACUUUGUGAAAUGACUU
miR7696a-3p	27,181.5	155,590.5	168,177.5	UUCAAAUGAGAACUUUGAAG
miR9767	0	96,130.5	131,227.5	GAUGGAAAGGACUUUGAAAAGA
miR2093-5p	0	89,975	80,110.5	GUGCUGUUACUUGGAAGAAA
miR5813	24,358.5	82,385.5	41,766	ACAGCAGGACGGUGGUCAUGGA
miR2916	13,876.5	79,125	73,311.5	UUGGGGGCUCGAAGACGAUCAGA
miR1520n	0	76,947.5	0	UCAACUCAGAACUGGUACGGACA
miR395x	0	51,046.5	0	GUGAAGUGUUCGGAUCGCU
miR7990b	0	49,339	0	GAAUAUUCAAAUGAGAACUUUG
miR5386	10,617	43,959.5	2505	CGUCGGCUGUCGGCGGACUG
miR4342	0	38,655	0	AAUGACUUGAGAGGUGUAGGAUAGGU
miR7532a	12,331	36,495.5	11,995.5	GAACAGCCUCUGGUCGAUGGA
miR2199	12,674.5	32,087.5	29,888.5	UGAUAACUCGACGGAUCGC
miR5568f-3p	9716.5	29,972	22,125.5	GUCUGGUAAUUGGAAUGAG
miR1026a	15,261	26,264.5	37,665.5	UGUGAAAUGACUUGAGAGGUA
miR3444a-5p	0	21,517.5	318	GUUGGGAGCUCGAAGACGAUCAGA
miR7545	4872	20,466.5	12,665	UUGAAGAAAUUAGAGUGCU
miR827-5p	0	16,313	13,833.5	UUUGUUUGAUGGUACCUACUC
miR8141	0	15,003.5	0	UCGUCUAGUAGCUGGUU
miR396a-5p	0	14,387	41,980.5	UUCCACAGCUUUCUUGAACUG
miR1110	0	10,075	4623	GCAGGGCGGUGGUCAUGGA
miR159a	324,743	9399.5	32,021.5	UUUGGAUUGAAGGGAGCUCUA
miR4994-3p	0	7722.5	12,323.5	UAAUUCUAGAGCUAAUACA
miR5671a	2145.5	5020.5	10,828	CAUGGUGGUGACGGGUGAC
miR166b	97,140	2943	3178	UCGGACCAGGCUUCAUUCCCC
miR159b-3p	74,369	2309	14,130.5	UUUGGAUUGAAGGGAGCUCUU
miR482b	59,366.5	2286.5	6964.5	UCUUACCUAUUCCUCCCAUGCC
miR1448	28,824	1770	3446.5	UCUUUCCAACGCCUCCCAUACU
miR7767-5p	18,941.5	1719.5	4330.5	CCAAGAUGAGUGCUCUCCC
miR482a-3p	15,428	916	1588	UUCCCAAUGCCGCCCAUUCCGA
miR2118	13,416.5	878.5	1304	UUGCCGAUUCCACCCAUUCCUA
miR472	27,541.5	827	8649.5	UUUCCUACCCCUCCCAUCCC
miR2118a-3p	12,621.5	727.5	1446.5	UUGCCGAUUCCACCCAUUCCU
miR162a-3p	12,305.5	427.5	4508.5	UCGAUAAACCUCUGCAUCCAG

Table 2. *Cont.*

miRNA	Read Count			Sequence (5′-3′)
	GSM	GSJ	GSS	
miR166m	18,156	343.5	331.5	UCGGACCAGGCUUCAUUCCCU
miR159f	22,346.5	75	1056	AACUGCCGACUCAUUCGUAC
miR396b-5p	37,325.5	0	0	UUCCACAGCUUUCUUGAACUU
miR1510a-5p	18,193	0	0	UUUCUUACCUAUUCCUCCCAUG
miR1077-5p	16,190.5	0	0	UUGAAGUGUUCGGAUCGCGGC
miR858-5p	13,839.5	0	5	UUCAUUGUCUGUUCGGCCGUA
miR2095-3p	0	0	82,480.5	CUUGGAUUUAUGAAAGUU
miR396b	0	0	50,319	UUCCACAGCUUUCUUGAACU
miR482a-5p	0	0	12,190.5	GGAAUGGGCUGUUUGGGAAGA
miR5037c	0	0	17,883.5	AGUGAGAACUUUGAAGGCCG
miR6194	0	0	69,261.5	UAGUAGGGAUUGACAGACUGAG
miR8682	0	0	47,369	AUAUCUCGGCUCUCGCAG
miR8752	0	0	20,994	UGAUGGGGAUAGGUCAUUGCA
miR9736	0	0	49,416.5	UGAAAGACAAACAACUGCG

Note: In the heatmap, GSM, GSJ, and GSS represent the highly expressed conservative miRNAs in May, July, and September, respectively.

Table 3. Known miRNAs that were specifically conserved in legumes from *Gleditsia sinensis*.

miRNA	Species	miRNA	Species
miR9762	*Glycine max*	*miR4995*	*Glycine max*
miR9748	*Glycine max*	*miR4994-3p*	*Glycine max*
miR9736	*Glycine max*	*miR4416a*	*Glycine max*
miR862b	*Glycine max*	*miR4415a-5p*	*Glycine max*
miR7545	*Lotus japonicus*	*miR4415a-3p*	*Glycine max*
miR7532a	*Lotus japonicus*	*miR4412-3p*	*Glycine max*
miR5780d	*Glycine max*	*miR4387d*	*Glycine max*
miR5770a	*Glycine max*	*miR4380b*	*Glycine max*
miR5741a	*Medicago truncatula*	*miR2670a*	*Medicago truncatula*
miR5678	*Glycine max*	*miR2658*	*Medicago truncatula*
miR5677	*Glycine max*	*miR2624*	*Medicago truncatula*
miR5672	*Glycine max*	*miR2619a*	*Medicago truncatula*
miR5671a	*Glycine max*	*miR2592bm-5p*	*Medicago truncatula*
miR5559-5p	*Medicago truncatula*	*miR2199*	*Medicago truncatula*
miR5282	*Medicago truncatula*	*miR1535a*	*Glycine max*
miR5258	*Medicago truncatula*	*miR1520n*	*Glycine max*
miR5209	*Medicago truncatula*	*miR1507a*	*Glycine max*
miR5208a	*Medicago truncatula*		*Vigna unguiculata*
miR5037c	*Glycine max*		*Glycine soja*
	Medicago truncatula		*Lotus japonicus*

3.4. Prediction of Novel miRNA Candidates in G. sinensis Pods

To further identify miRNAs in *G. sinensis*, the unannotated sRNA sequences were predicted in order to identify novel miRNAs of *G. sinensis* pods. According to strict selection rules, 59 sequences belonging to 37 families were predicted to be novel miRNAs with typical stem-loop structures (Table S4 and Figure S2). Among them, 28 novel miRNAs with 15 miRNAs were expressed in GSM, 27 novel miRNAs with 5 miRNAs were expressed in GSJ, and 32 novel miRNAs with 14 miRNAs were expressed in GSS, respectively. In total, 25 miRNAs had corresponding miRNAs, which were proved to be bona-fide miRNAs (Table S4). The miRNAs of the remaining 34 predicted miRNAs were not found owing to the limited sequencing depth or other causes; however, all of these miRNAs had a perfect typical stem-loop structure (Figure S2). After matching these miRNAs in miRBase (version 22.0), only 11 novel miRNAs could be partially matched with those of other plants (Table 4).

Table 4. Novel miRNAs (part) identified in *G. sinensis* pods.

miRNA	Sequence (5′-3′)	Precursor Length (nt)	MFE	Read Count		
				GSM	GSJ	GSS
gsi-smR1	CCUUCUCUUCCAUUCUUCUAG	226	−59.7	72	0	133.5
gsi-smR5	UUGGACUCUCUUCUUCUCAUG	148	−85.3	41.5	2.5	206
gsi-smR6	UCUUACCCACACCACCUAGCCC	300	−97.2	1139	60	182.5
gsi-smR7	UGCAGAACAAGUCCCAGCUUU	211	−68.6	0	20	2.5
gsi-smR9	AAGAACUCUUAUACCAAUUCG	103	−51.1	0	0	11
gsi-smR10	UGGACUCUCUUCUUCUCAUG	143	−82	0	0	63
gsi-smR25	AAGUUGAGAACAUUGAUGGC	120	−49.4	0	2.5	3
gsi-smR34	UGGUGAUCACGGGAUGAAGCU	226	−79.1	571.5	8.5	0
gsi-smR35	UGGUGAUCACGGGAUGAAGCU	349	−118.4	0	11.5	0
gsi-smR54	UUUUCGUCUUCGAGUUUCUUA	254	−108.6	1134	18	392.5
gsi-smR55	UUUUCGUCUUCGAGUUUCUUA	235	−99.4	1886	0	28.5

3.5. Expression Analysis of miRNAs Identified in G. sinensis Pods

To identify whether these miRNAs are involved in the regulation of saponin synthesis in *G. sinensis* pods, the expression of 74 known miRNAs was analyzed in three developmental stages of the pods (Table S5). The results demonstrated that many differentially expressed miRNAs (DEM) in *G. sinensis* were expressed in special periods during the pods' development. For instance, the expression of *miR9767* was the highest in July and September, while the expression of *miR396b-3p* was the highest in May. In total, the number of upregulated miRNAs was almost consistent with that of downregulated miRNAs from May to July. Intriguingly, with the development of the pods, the number of upregulated miRNAs was much higher than that of downregulated miRNAs from July to September (Figure 4). For example, highly expressed *miR2095-3p*, *miR396b*, and *miR6194* were significantly upregulated in September; meanwhile, *miR2093-5p* was dramatically induced in July (the most abundant DEM with 89,975 reads) and September (the third most abundant DEM with 80,110.5 reads). Furthermore, the expression of some miRNAs showed different trends in different periods. For example, *miR838-3p* and *miR4415a-3p* were significantly downregulated from May to July but were upregulated from July to September (Table S5).

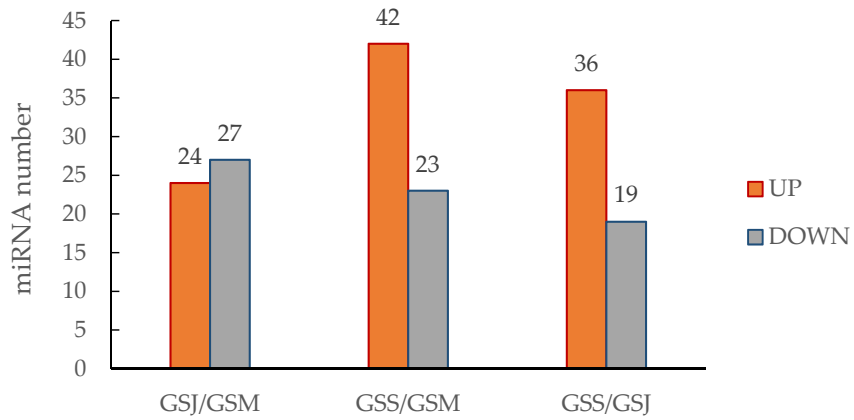

Figure 4. Differentially expressed miRNA numbers in three groups of *Gleditsia sinensis* pods. Note: GSM: *G. sinensis* pods in May; GSJ: *G. sinensis* pods in July; GSS: *G. sinensis* pods in September.

3.6. Target Prediction of miRNAs with Differential Expression

To better understand the function of DEM, 708 targets from 37 differentially expressed miRNAs were predicted (Table S6). For the different developmental stages of *G. sinensis* pods, 23 miRNAs with 430 targets were detected in GSJ/GSM, 28 miRNAs with 459 targets were detected in GSS/GSM, and 8 miRNAs with 239 targets were detected in GSS/GSJ (Figure 5). Among them, there were 64 unigenes targeted by 6 legume-specific miRNAs (Tables 3 and S6). According to the annotation of the targets, most of the targets were predicted to encode resistant proteins and diverse transcription factors, while a small number had no annotation information (Table S7). Interestingly, targets encoding enzymes in secondary metabolic pathways were also obtained. For example, *CL3189.Contig4* targeted by *miR5037a* encodes the enzyme of GGPS (geranylgeranyl diphosphate synthase) that might consume the intermediate of GPP during saponin biosynthesis. Then, five targets (*CL1552.Contig7*, *CL1552.Contig6*, *CL1552.Contig2*, *CL1552.Contig10*, and *CL1552.Contig1l*) recognized by *miR838-3p* belonged to P450 family genes, which are important regulatory factors for the decoration of the pentacyclic skeleton in the last step of saponin biosynthesis. These miRNAs have been shown to regulate the growth and development of *G. sinensis* pods and saponin biosynthesis. For instance, *miR858a* regulated anthocyanin synthesis by inhibiting the expression of MYB, a translation-inhibiting transcription factor involved in anthocyanin synthesis [20,31]. In addition, *miR156* had a positive regulatory effect on anthocyanin biosynthesis by targeting SPL [32] and was also related to the content of gallated catechins [33]. As expected, in our investigation, *miR858* and *miR156* were both detected to be changed differentially in *G. sinensis* pods, further supporting their conserved roles in the regulation of terpenoid synthesis in plants.

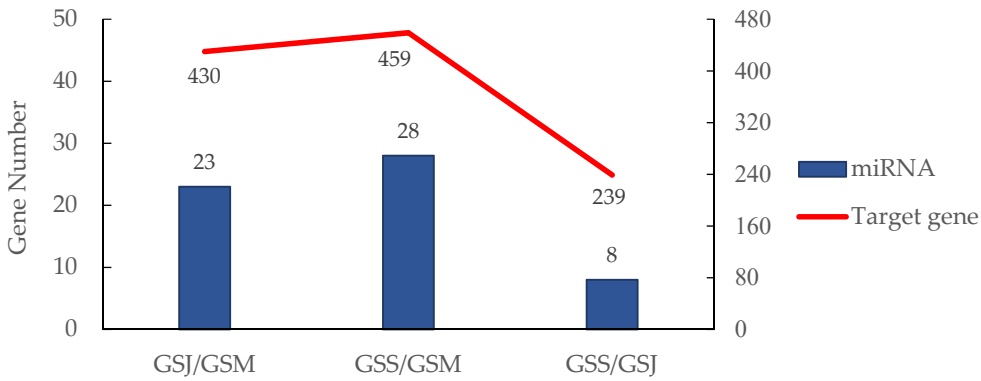

Figure 5. The number of differentially expressed miRNAs with targets in three comparison groups of *Gleditsia sinensis*. Note: GSM: *G. sinensis* pods in May; GSJ: *G. sinensis* pods in July; GSS: *G. sinensis* pods in September.

3.7. GO Analysis of Targets of Differentially Expressed miRNAs

To further annotate the function of the targets of DEM, GO analysis was further conducted. We found that the terms of geranyl-diphosphate geranyl-acyltransferase activity (GO: 0016767) and phytoene synthase activity (GO: 0004337) were prominently enriched from May to September (Figure S3). Moreover, the term of geranyl transferase activity (GO: 0004337) was also rich in higher levels from July to September. According to previous studies, the unigenes in these three terms are related to the anabolism of geranyl diphosphate (GPP) or geranylgeranyl diphosphate (GGPP). The biological process indicated that most of the targets were predicted to participate in responding to the induction and transporting protein from May to July. Whereas most of the targets were predicted to be related to the function of the vesicle from July to September (Figure S3), including vesicle localization from the rough endoplasmic reticulum to the Golgi body (vesicle targeting, rough ER to cis-Golgi, GO: 0048207) and COP modification on budding vesicles (COPII-coated vesicle budding, GO: 0090114).

3.8. KEGG Analysis of Targets of Differentially Expressed miRNAs

To analyze the pathways of the targets of DEM, KEGG enrichment was further performed. We found that the terpene skeleton pathway, brassinosteroid biosynthesis (BRB), indole alkaloid biosynthesis (IAB), zeatin biosynthesis (ZTB), and carotenoid biosynthesis (CTB) were enriched. More interestingly, most of these pathways were required for terpenoid backbone biosynthesis from May to September (Figure S4). Among them, BRB was one of the most enriched pathways, including the targets of *miR838-3p* in all the developmental stages. However, IAB, including the targets of *miR2093-5p*, and terpenoid backbone biosynthesis (TBB), including the targets of *miR4414b*, were among the top 20 enrichment pathways from May to July, while these targets were not enriched from July to September.

4. Discussion

4.1. Legume-Specific miRNAs in Gleditsia sinensis

In this investigation, 57 legume-specific miRNAs were found in *G. sinensis*, which provides further molecular proof of the molecular classification of *G. sinensis* as Leguminosae plants. Among nine miRNAs with differential expression in pods during different developmental stages, the targets of *miR2658*, *miR4414b*, *miR4415a-3p*, *miR4994-3p*, *miR5213-5p*, and *miR9736* were ranked in the top 20 GO or KEGG enrichment pathways (Table S5, Figures S3 and S4). Interestingly, the target annotation showed that many of these miRNAs were involved in stress responses. For example, *miR5213-5p* was induced from May to July, and its targets were predicted to regulate phytochelatin biosynthetic/metabolic processes in response to heavy-metal stress [34] and plant–pathogen interaction pathways. The result was similar to that of previous reports in that *miR5213-5p* could regulate abiotic stress by targeting NBS-LRR genes [35]. In plant–pathogen interaction pathways, it was shown that other targets of *miR5213-5p* belong to genes encoding NBS-LRR-family proteins produced to resist pathogenic stress [36], implying that *miR5213-5p* might negatively regulate the response to pathogen infection. Similarly, *miR4414b* was also suggested to be related to the plant–pathogen interaction pathway. Additionally, some of the remaining legume-specific miRNAs with no differential expression in *G. sinensis* might also be involved in abiotic or biotic stress responses. For example, *miR5368* and *miR3512* were found to respond to drought stress in alfalfa [35]. Through degradome sequencing, *miR9748* was validated as targeting genes encoding HSP90 (heat-shock protein) and the transcription factor *MYC2* to respond to selenium hyperaccumulation [37]. *miR1507a* was reported to be involved in the resistance of soybeans to pathogen infection by regulating several NBS-LRR-family disease resistance genes during ETI [38]. However, the function of some species-specific miRNAs in this investigation was not annotated due to the incomplete genome of *G. sinensis*; nevertheless, the regulatory roles of these miRNAs were reported in other plants. For example, *miR5559* was shown to respond to water stress in Caragana korshinskii in the Loess Plateau [39] and could regulate chilling injury [40].

The overexpression of *gma-miR1510a/b* could reduce resistance to Phytophthora sojae by suppressing the expression of NBS-LRR genes [41]. Thus far, in Leguminosae, the molecular mechanism of these legume-specific miRNAs, which are involved in the response to multiple stresses for adaption for better growth, could not be explained, especially in *G. sinensis*, a perennial woody plant.

Intriguingly, another molecular proof that supports *G. sinensis* being classified as a legume is the existence of the miRNAs in *G. sinensis* related to symbiotic process, which exist widely in *Leguminosae*. *miR4416* was reported to regulate the nodule number by targeting *GmRIP1* (rhizobium-induced peroxidase 1 (RIP1)-like peroxidase gene) [42]. In addition, thus far there are no reports that nitrogen-fixing rhizobium exists in *G. sinensis*; however, there might be other beneficial symbiotic bacteria for better survival, adaption, and growth of *G. sinensis*, which could be supported by the annotation that one of the targets of *miR4414b* in *G. sinensis* was suggested to be involved in intracellular protein transport in a symbiotic interaction.

Moreover, we found that *miR862b*, *miR5671a*, *miR5037c*, *miR2089-3p*, and *miR1520n* might only be conserved in legumes, but other members in these families could be found in non-legume species [43–47].

4.2. miRNAs Involved in the Development of G. sinensis Pods

Thus far, diverse miRNAs have been validated as playing indispensable roles in plant development, for instance, *miR156*, *miR159*, *miR160*, *miR163*, *miR164*, *miR165*, *miR166*, *miR167*, *miR171*, and *miR172* were showed to regulate pods, seeds, root development, and phase transitions (Table S8). In this investigation, *miR156*, *miR166*, and miR396 were differentially expressed in *G. sinensis* pods with different developmental stages. Among them, the expression of the total members in the *miR396* family generally exceeded the other two miRNA families. However, *miR396*, with six members, was expressed differently in the three stages (Table S3). Intriguingly, we found that *miR396b-5p* and *miR396b-3p* were the most abundant during the early stage of pod development but dramatically decreased in the latter two stages. Conversely, *miR396a* was highly expressed in the third stage (Table S6). A similar expression pattern was also found in the *miR156* family in *G. sinensis*, suggesting that different members in same family may have different roles in the process of pod development.

According to GO annotation and KEGG enrichment analysis, the targets of *miR396b*, *miR396b-3p*, and *miR156d-3p* were enriched in the top 20 molecular functions, biological processes, or metabolic pathways (Figures S3 and S4). The *miR396* family, conserved among *A. thaliana*, *Populus trichocarpa*, and *Medicago truncatula,* was reported to regulate the development of leaves, seedlings, pods, and flowers by suppressing the targets encoding GRFs (growth-regulating factors) [48–51]. In the model legume *Medicago truncatula*, *miR396b* was demonstrated to reduce root growth and mycorrhizal associations by targeting six GRFs and two *bHLH79*-like target genes [51]. Since the genome of *G. sinensis* was unavailable, based on the transcription sequence, the target of *miR396b* from the pods was enriched in Golgi vesicle budding, lipid translocation, and membrane budding. *miR156d-3p* was enriched in plant hormone signal transduction, and its targets were predicted to encode auxin response factor 18-like (ARF, gene ID: *G. sinensis* Unigene1136, unpublished transcriptome data). In *Solanum lycopersicum* L., miR156 was predicted to target *SPL/SBP* to negatively regulate fruit development [52]. However, *miR156d-3p* may have a different regulation module for pod development in *G. sinensis*.

It is well known that RNA-binding proteins (RBPs) and miRNAs are regarded as important factors for the suppression of the expression of mRNAs affecting multiple cellular functions during mRNA post-transcription processes [53,54]. Polyadenylation is a two-step nuclear process including cleavage of the pre-mRNA at the 3′-end and the polymerization of a polyadenosine (polyA) tail to promote mRNA stability [55]. However, polyadenylation, which widely occurs during the degradation of intermediates and the production of polyA, further promotes mRNA degradation [56]. AU-rich elements (AREs)

that can bind to the target genes of *miR2658* are a kind of cis-acting destabilizing elements that dictate mRNA degradation [57]. In this investigation, *miR2658* was highly expressed in May and was predicted to regulate the polyadenylation-dependent mRNA catabolic process, implying that *miR2658* might regulate the ARE-mediated mRNA delay. Moreover, *miR2658* was only expressed selectively in May, which might better regulate the growth and development of pod tissues.

Furthermore, the targets of *miR9736* were also significantly enriched in the KEGG pathway of photosynthesis and plant-pathogen interactions (Figure S3). Similar to the reduction in *miR156* that changes the time of vegetative phase by increasing photosynthesis [58], *miR9736*, with a sharp increase in September, might change vegetative development in *G. sinensis* pods. Overall, as prevalent development regulators, *miR396*, *miR156*, *miR2658*, *miR829*, and *miR9736* may also regulate the development of pods in different aspects.

4.3. miRNAs Involved in Terpenoid Synthesis of Gleditsia sinensis Pods

Brassinosteroids (BR) synthesized from squalene and then cyclized to become cycloartenol are a kind of terpene with biological activity. They were also identified as an endogenous steroid hormone that promotes plant growth and development [59]. For example, BR was reported to regulate the stabilization of microtubules to regulate plant pavement cells and leaf growth [60]. Thus far, only *miR1848*, which modulates the quality of seeds by cleaving *OsCYP51G3*, has been proved to regulate brassinosteroid biosynthesis in rice [61]. On the other hand, *miR172* could control the BR sensitivity of plants by regulating *BAK1* in BR signaling [62]. In this investigation, the target of *miR838-3p*, which was enriched in the BR pathway, encodes the enzyme of PHYB activation tagged suppressor 1 (*CYP734A1*, *BAS1*). In addition, *miR838-3p* was only expressed in May and September, and the expression in September was more than that in May. This implied that *miR838-3p* might suppress the oxidoreduction of brassinosteroids to promote the production and regulate the biosynthesis of brassinosteroids in different developmental stages of *G. sinensis* pods (Figure 6).

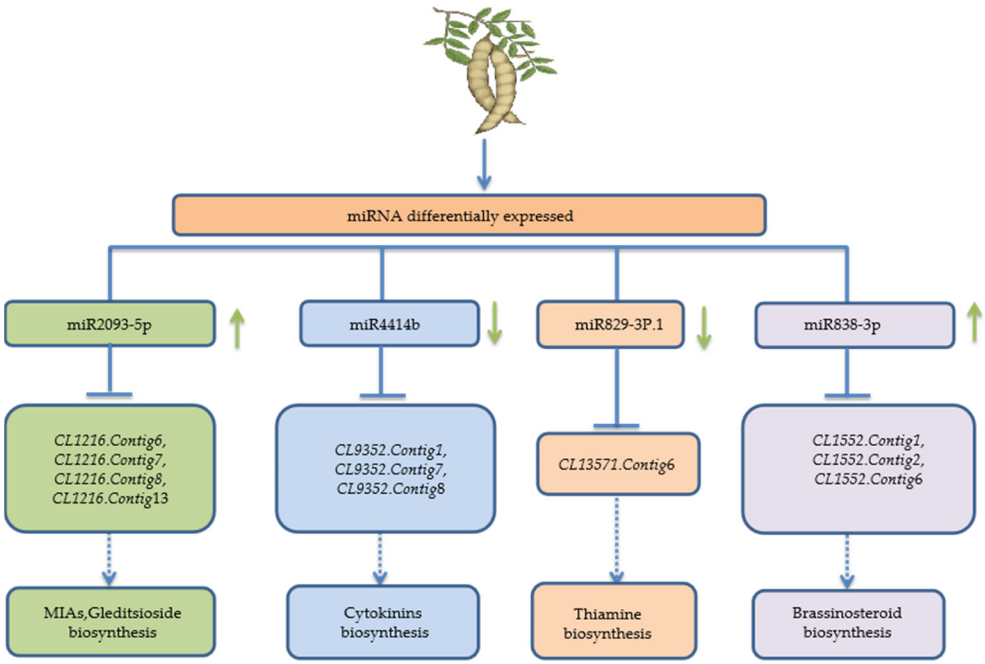

Figure 6. Differential expression of miRNAs in the synthesis of terpenoids of *Gleditsia sinensis*. Note: The upward arrow indicates upregulation of miRNAs; the downward arrow indicates downregulation of miRNAs, and the dotted arrow represents miRNAs indirectly involved in the synthesis of related terpenoids by inhibiting the expression of target genes.

Thiamine, called vitamin B1, is a vital cofactor for plant development and growth. In wheat, thiamine thiazole synthase was enriched, underlying the vernalization response [63]. In oil palm seedlings, thiamine biosynthesis was enhanced by endophytic colonization [64]. In soybean, thiamine was increased as ROS signaling after injection of *Rhizoctonia solani* [65]. It was demonstrated that *miR829* could resist *Exserohilum turcicum* in maize [66]. In this study, *miR829-3p.1* was highly expressed in May but dropped to zero in July and was then upregulated in September. Additionally, the targets of *miR829-3p.1* were predicted to take part in thiamine biosynthesis (Tables S5 and S6).

In addition, the IAB pathway related to the development of saponin was enriched. IAB, which is derived from tryptophan with secologanin, is an important secondary metabolite [67]. In *Catharanthus roseus*, large numbers of monoterpene indole alkaloids (MIAs) have been identified to possess pharmacological activities, such as anticancer activity. In this study, four target genes of *mir2093-5p* (*CL1216.Contig13*, *CL1216.Contig6*, *CL1216.Contig7*, and *CL1216.Contig8*) were predicted to encode the enzyme of polyneuridine-aldehyde esterase (PNAE) in the IAB process (Figure 6). However, *miR2093-5p* was largely expressed in July and September, implying that indole alkaloids might be abundantly produced at an early stage. It was then significantly inhibited by *miR2093-5p*, possibly to reduce the consumption of tryptophan and provide a substrate for the synthesis of other essential protein components in plants. On the other hand, the accumulation of saponins may be regulated by feedback. The pathway of IAB shared the terpenoid backbone biosynthesis with other terpenoids, such as triterpenoids. Hence, this miRNA mechanism could balance the contents of the production of various terpenoids and play different roles at each stage. Additionally, the indole zeatin biosynthesis (ZTB) pathway was also enriched. The enriched targets of *miR838-3p* were *cl1552.contig1*, *cl1552.contig2,* and *cl1552.contig6* encoding the BAS1 enzyme in the BRB pathway and belonging to the P450 family (Figure 6). The enriched target genes of *miR4414b* were *cl9352.Contig1*, *cl9352.Contig7,* and *cl9352.Contig8* encoding IPT. These miRNAs should negatively regulate these terpenoid pathways by regulating the catalytic enzyme genes.

5. Conclusions

A total of 351 conserved miRNAs belonging to 216 families were identified in *Gleditsia sinensis* pods at different developmental stages, which showed that the saponins increased gradually from May to September. A total of 36 conserved miRNAs existed specifically in legumes. A total of 708 unigenes were predicted to be the targets of 37 differentially expressed miRNAs. The targets of these differentially expressed miRNAs were involved in the regulation of terpenoid biosynthesis. To date, this is the first report of miRNA identification in *G. sinensis* and miRNA expression profiles at different developmental stages of the pod, which provides a basis for uncovering the molecular regulation of saponin synthesis in *G. sinensis* and new insights into the role of miRNAs in legumes.

Supplementary Materials: The following are available online at: https://www.mdpi.com/article/10.3390/f13010108/s1, Figure S1: The concentrations of saponins in three stages (May, July, and September) were quantified by spectrophotometry colorimetry with echinocystic acid (EA). (a) Full wavelength scanning of EA and methanol extract of pods from June to November. (b) Standard curve of echinocystic acid (EA) from 20 μg to 100 μg. Figure S2: Secondary structure of novel miRNAs (green represents the mature sequence of novel miRNA; yellow represents the corresponding star sequence of novel miRNA). Figure S3: GO enrichment of target genes in May vs. July and July vs. September. Figure S4: Top 20 KEGG enrichment pathways of target genes in July/May (a) and September/July (b) from *Gleditsia sinensis* pods. Table S1: Saponin content and absorbance of *Gleditsia sinensis* pods and leaves at different stages. Table S2: Known miRNAs from three developmental periods in *Gleditsia sinensis* pods. Table S3: Known miRNA families from three periods of *Gleditsia sinensis* pods. Table S4: Novel miRNA from three periods of *Gleditsia sinensis* pods. Table S5: Differentially expressed miRNAs from three development periods of *Gleditsia sinensis* pods. Table S6: Predicted target number of differentially expressed miRNAs in *Gleditsia sinensis* pods. Table S7: Predicted target

number of differentially expressed miRNAs in *Gleditsia sinensis* pods. Table S8: miRNAs involved in development and the annotation of their targets.

Author Contributions: Y.Y. and J.W. were responsible for conceptualization, bioinformatic analysis, data interpretation and drafting the manuscript. C.W. and H.C. assisted in the statistical analysis and critical evaluation of manuscripts. Y.L. was responsible for sorting out the forms. Y.W. and W.G. was responsible for supervision, project administration and funding acquisition to support this research. All authors have read and agreed to the published version of the manuscript.

Funding: This work was supported by the National Natural Science Foundation of China (32071504 and 31670671), the Fundamental Research Funds for the Central Universities (2016ZCQ05) and the Special Support Project of Development and Planning Division of Beijing Forestry University (2018FGC08).

Data Availability Statement: sRNA sequencing data could be available at the NCBI SRA database (http://www.ncbi.nlm.nih.gov/sra, accessed on 26 November 2021) with the accession numbers PRJNA783670, PRJNA783672, and PRJNA783674.

Acknowledgments: We thank the reviewers and editors for the thoughtful comments and suggestions on the manuscript. We thank the 1 GENE company for helping with sRNA-sequencing and technical assistance.

Conflicts of Interest: The authors declare that the research was conducted in the absence of any commercial or financial relationships that could be construed as a potential conflict of interest.

References

1. Zhang, J.P.; Tian, X.H.; Yang, Y.X.; Liu, Q.X.; Wang, Q.; Chen, L.P.; Li, H.L.; Zhang, W.D. Gleditsia species: An ethnomedical, phytochemical and pharmacological review. *J. Ethnopharmacol.* **2016**, *178*, 155–171.
2. Liang, J.Y.; An, X.N.; Jiang, J.X.; Zhu, L.W.; Zhang, W.M. Study on the chemical constituents of the pod of *G. sinensis*. *Chin. Wild Plant Resour.* **2003**, *22*, 44–46.
3. Lian, X.Y.; Zhang, Z. Quantitive analysis of gleditsia saponins in the fruits of *G. sinensis* Lam. by high performance liquid chromatography. *J. Pharm. Biomed. Anal.* **2013**, *75*, 41–46.
4. Jin, S.K.; Yang, H.S.; Choi, J.S. Effect of *G. sinensis* Lam. Extract on physico-chemical properties of emulsion-type pork sausages. *Korean J. Food Sci. Anim. Resour.* **2017**, *37*, 274–287.
5. Kim, K.H.; Han, C.W.; Yoon, S.H.; Kim, Y.S.; Kim, J.I.; Joo, M.; Choi, J.Y. The fruit hull of *G. sinensis* enhances the anti-tumor effect of cis-diammine dichloridoplatinum II (Cisplatin). *Evid.-Based Complement. Altern. Med.* **2016**, *2016*, 7480971.
6. Kim, Y.; Koh, J.H.; Ahn, Y.J.; Oh, S.; Kim, S.H. The synergic anti-inflammatory impact of *G. sinensis* Lam. and Lactobacillus brevis KY21 on intestinal epithelial cells in a DSS-induced colitis model. *Korean J. Food Sci. Anim. Resour.* **2015**, *35*, 604–610. [PubMed]
7. Kuwahara, Y.; Nakajima, D.; Shinpo, S.; Nakamura, M.; Kawano, N.; Kawahara, N.; Yamazaki, M.; Saito, K.; Suzuki, H.; Hirakawa, H. Identification of potential genes involved in triterpenoid saponins biosynthesis in *Gleditsia sinensis* by transcriptome and metabolome analyses. *J. Nat. Med.* **2019**, *73*, 369–380. [PubMed]
8. Zhao, S.; Wang, L.; Liu, L.; Liang, Y.; Sun, Y.; Wu, J. Both the mevalonate and the non-mevalonate pathways are involved in ginsenoside biosynthesis. *Plant Cell Rep.* **2014**, *33*, 393–400. [PubMed]
9. Thimmappa, R.; Geisler, K.; Louveau, T.; O'Maille, P.; Osbourn, A. Triterpene biosynthesis in plants. *Annu. Rev. Plant Biol.* **2014**, *65*, 225–257. [PubMed]
10. Seki, H.; Tamura, K.; Muranaka, T. P450s and UGTs: Key players in the structural diversity of triterpenoid saponins. *Plant Cell Physiol.* **2015**, *56*, 1463–1471.
11. Lange, B.M.; Ghassemian, M. Genome organization in *Arabidopsis thaliana*: A survey for genes involved in isoprenoid and chlorophyll metabolism. *Plant Mol. Biol.* **2003**, *51*, 925–948. [PubMed]
12. Sakakibara, H. Cytokinins: Activity, biosynthesis, and translocation. *Annu. Rev. Plant Biol.* **2006**, *57*, 431–449. [PubMed]
13. Qiu, L.; Qi, Y.; Wang, M.; Jia, X. Relationship between secondary metabolite autotoxic to plant and continuous cropping obstacles. *Soils* **2010**, *42*, 1–7.
14. Fan, R.; Li, Y.; Li, C.; Zhang, Y. Differential microRNA analysis of glandular trichomes and young leaves in Xanthium strumarium L. reveals their putative roles in regulating terpenoid biosynthesis. *PLoS ONE* **2015**, *10*, e0139002.
15. Gupta, O.P.; Karkute, S.G.; Banerjee, S.; Meena, N.L.; Dahuja, A. Contemporary understanding of miRNA-based regulation of secondary metabolites biosynthesis in plants. *Front. Plant Sci.* **2017**, *29*, 374.
16. Soto-Suarez, M.; Baldrich, P.; Weigel, D.; Rubio-Somoza, I.; San, S.B. The *Arabidopsis* miR396 mediates pathogen-associated molecular pattern-triggered immune responses against fungal pathogens. *Sci. Rep.* **2017**, *7*, 44898.
17. Smoczynska, A.; Szweykowska-Kulinska, Z. MicroRNA-mediated regulation of flower development in grasses. *Acta Biochim. Pol.* **2016**, *63*, 687–692.

18. Wang, Y.; Zou, W.; Xiao, Y.; Cheng, L.; Liu, Y.; Gao, S.; Shi, Z.; Jiang, Y.; Qi, M.; Xu, T.; et al. MicroRNA1917 targets CTR4 splice variants to regulate ethylene responses in tomato. *J. Exp. Bot.* **2018**, *69*, 1011–1025. [PubMed]
19. Hou, Y.; Zhai, L.; Li, X.; Xue, Y.; Wang, J.; Yang, P.; Cao, C.; Li, H.; Cui, Y.; Bian, S. Comparative analysis of fruit ripening-related miRNAs and their targets in blueberry using small RNA and degradome sequencing. *Int. J. Mol. Sci.* **2017**, *18*, 2767.
20. Wang, Y.; Wang, Y.; Song, Z.; Zhang, H. Repression of *MYBL2* by both microRNA858a and HY5 leads to the activation of anthocyanin biosynthetic pathway in *Arabidopsis*. *Mol. Plant* **2016**, *9*, 1395–1405. [PubMed]
21. Kajal, M.; Singh, K. Small RNA profiling for identification of miRNAs involved in regulation of saponins biosynthesis in *Chlorophytum borivilianum*. *BMC Plant Biol.* **2017**, *17*, 265.
22. Chang, S.; Puryear, J.; Cairney, J. A simple and efficient method for isolating RNA from pine trees. *Plant Mol. Biol. Rep.* **1993**, *11*, 113–116.
23. Hou, J.; Sun, F.S.; Wu, Q.M.; Yang, Y.; He, W.; Wang, Y.W. An efficient method for total RNA extraction of poplar bark infected with pathogen and the application. *Plant Physiol. J.* **2014**, *50*, 223–228.
24. Zhai, R.; Feng, Y.; Wang, H.; Zhan, X.; Shen, X.; Wu, W.; Zhang, Y.; Chen, D.; Dai, G.; Yang, Z.; et al. Transcriptome analysis of rice root heterosis by RNA-Seq. *BMC Genom.* **2013**, *14*, 19.
25. Meyers, B.C.; Axtell, M.J.; Bartel, B.; Bartel, D.P.; Baulcombe, D.; Bowman, J.L.; Cao, X.; Carrington, J.C.; Chen, X.; Green, P.J.; et al. Criteria for annotation of plant microRNAs. *Plant Cell* **2008**, *20*, 3186–3190.
26. Allen, E.; Xie, Z.; Gustafson, A.M.; Carrington, J.C. microRNA-directed phasing during trans-acting siRNA biogenesis in plants. *Cell* **2005**, *121*, 207–221. [PubMed]
27. Dai, X.; Zhao, P.X. psRNATarget: A plant small RNA target analysis server. *Nucleic Acids Res.* **2011**, *39*, 155–159.
28. Kanehisa, M.; Araki, M.; Goto, S.; Hattori, M.; Hirakawa, M.; Itoh, M.; Katayama, T.; Kawashima, S.; Okuda, S.; Tokimatsu, T.; et al. KEGG for linking genomes to life and the environment. *Nucleic Acids Res.* **2008**, *36*, 480–484.
29. Ren, Y.Y.; Chen, L.; Zhang, Y.Y.; Kang, X.Y.; Zhang, Z.Y.; Wang, Y.W. Identification and characterization of salt-responsive microRNAs in *Populus tomentosa* by high-throughput sequencing. *Biochimie* **2015**, *15*, 93–105.
30. Wang, X.; Zheng, Y.Q.; Su, S.C.; Ao, Y. Discovery and profiling of microRNAs at the critical period of sex differentiation in *Xanthoceras sorbifolium* Bunge. *Forests* **2019**, *10*, 1141.
31. Jia, X.; Shen, J.; Liu, H.; Li, F.; Ding, N.; Gao, C.; Pattanaik, S.; Patra, B.; Li, R.; Yuan, L. Small tandem target mimic-mediated blockage of microRNA858 induces anthocyanin accumulation in tomato. *Planta* **2015**, *242*, 283–293.
32. Gou, J.Y.; Felippes, F.F.; Liu, C.J.; Weigel, D.; Wang, J.W. Negative regulation of anthocyanin biosynthesis in *Arabidopsis* by a miR156-targeted SPL transcription factor. *Plant Cell* **2011**, *23*, 1512–1522. [PubMed]
33. Li, H.; Lin, Q.; Yan, M.; Wang, M.; Wang, P.; Zhao, H.; Wang, Y.; Ni, D.; Guo, F. Relationship between Secondary Metabolism and miRNA for Important Flavor Compounds in Different Tissues of Tea Plant (*Camellia sinensis*) As Revealed by Genome-Wide miRNA Analysis. *J. Agric. Food Chem.* **2021**, *69*, 2001–2012.
34. Zhang, X.; Rui, H.; Zhang, F.; Hu, Z.; Xia, Y.; Shen, Z. Overexpression of a functional Vicia sativa PCS1 homolog increases cadmium tolerance and phytochelatins synthesis in *Arabidopsis*. *Front. Plant Sci.* **2018**, *9*, 107.
35. Li, Y.; Wan, L.; Bi, S.; Wan, X.; Li, Z.; Cao, J.; Tong, Z.; Xu, H.; He, F.; Li, X. Identification of drought-responsive microRNAs from roots and leaves of alfalfa by high-throughput sequencing. *Genes* **2017**, *8*, 119.
36. Gururani, M.A.; Venkatesh, J.; Upadhyaya, C.P.; Nookaraju, A.; Pandey, S.K.; Park, S.W. Plant disease resistance genes: Current status and future directions. *Physiol. Mol. Plant Pathol.* **2012**, *78*, 51–65.
37. Cakir, O.; Candar-Cakir, B.; Zhang, B. Small RNA and degradome sequencing reveals important microRNA function in *Astragalus chrysochlorus* response to selenium stimuli. *Plant Biotechnol. J.* **2016**, *14*, 543–556. [PubMed]
38. Bao, D.; Ganbaatar, O.; Cui, X.; Yu, R.; Bao, W.; Falk, B.W.; Wuriyanghan, H. Down-regulation of genes coding for core RNAi components and disease resistance proteins via corresponding microRNAs might be correlated with successful Soybean mosaic virus infection in soybean. *Mol. Plant Pathol.* **2018**, *19*, 948–960.
39. Ning, P.; Zhou, Y.; Gao, L.; Sun, Y.; Zhou, W.; Liu, F.; Yao, Z.; Xie, L.; Wang, J.; Gong, C. Unraveling the microRNA of *Caragana korshinskii* along a precipitation gradient on the Loess Plateau, China, using high-throughput sequencing. *PLoS ONE* **2017**, *12*, e172017.
40. Zhang, S.; Wang, Y.; Li, K.; Zou, Y.; Chen, L.; Li, X. Identification of cold-responsive miRNAs and their target genes in nitrogen-fixing nodules of soybean. *Int. J. Mol. Sci.* **2014**, *15*, 13596–13614.
41. Cui, X.; Yan, Q.; Gan, S.; Xue, D.; Dou, D.; Guo, N.; Xing, H. Overexpression of gma-miR1510a/b suppresses the expression of a NB-LRR domain gene and reduces resistance to *Phytophthora sojae*. *Gene* **2017**, *621*, 32–39.
42. Yan, Z.; Hossain, S.; Valdés-López, O.; Hoang, N.T.; Zhai, J.; Wang, J.; Libault, M.; Brechenmacher, L.; Findley, S.; Joshi, T.; et al. Identification and functional characterization of soybean root hair microRNAs expressed in response to *Bradyrhizobium japonicum* infection. *Plant Biotechnol. J.* **2016**, *14*, 332–341.
43. Xie, F.; Wang, Q.; Sun, R.; Zhang, B. Deep sequencing reveals important roles of microRNAs in response to drought and salinity stress in cotton. *J. Exp. Bot.* **2015**, *66*, 789–804. [PubMed]
44. Wang, Y.; Zhang, C.; Hao, Q.; Sha, A.; Zhou, R.; Zhou, X.; Yuan, L. Elucidation of miRNAs-mediated responses to low nitrogen stress by deep sequencing of two soybean genotypes. *PLoS ONE* **2013**, *8*, e67423.
45. Lin, Y.; Lai, Z. Comparative analysis reveals dynamic changes in miRNAs and their targets and expression during somatic embryogenesis in longan (*Dimocarpus longan* Lour.). *PLoS ONE* **2013**, *8*, e60337.

46. Lu, Y.B.; Qi, Y.P.; Yang, L.T.; Guo, P.; Li, Y.; Chen, L.S. Boron-deficiency-responsive microRNAs and their targets in *Citrus sinensis* leaves. *BMC Plant Biol.* **2015**, *15*, 271.
47. Su, Y.; Zhang, Y.; Huang, N.; Liu, F.; Su, W.; Xu, L.; Ahmad, W.; Wu, Q.; Guo, J.; Que, Y. Small RNA sequencing reveals a role for sugarcane miRNAs and their targets in response to *Sporisorium scitamineum* infection. *BMC Genom.* **2017**, *18*, 325.
48. Cao, D.; Wang, J.; Ju, Z.; Liu, Q.; Li, S.; Tian, H.; Fu, D.; Zhu, H.; Luo, Y.; Zhu, B. Regulations on growth and development in tomato cotyledon, flower and fruit via destruction of miR396 with short tandem target mimic. *Plant Sci.* **2016**, *247*, 1–12.
49. Liu, D.; Song, Y.; Chen, Z.; Yu, D. Ectopic expression of miR396 suppresses GRF target gene expression and alters leaf growth in *Arabidopsis*. *Physiol. Plant.* **2009**, *136*, 223–236. [PubMed]
50. Baucher, M.; Moussawi, J.; Vandeputte, O.M.; Monteyne, D.; Mol, A.; Pérez-Morga, D.; El Jaziri, M. A role for the miR396/GRF network in specification of organ type during flower development, as supported by ectopic expression of *Populus trichocarpa* miR396c in transgenic tobacco. *Plant Biol.* **2013**, *15*, 892–898.
51. Bazin, J.; Khan, G.A.; Combier, J.P.; Bustos-Sanmamed, P.; Debernardi, J.M.; Rodriguez, R.; Sorin, C.; Palatnik, J.; Hartmann, C.; Crespi, M.; et al. miR396 affects mycorrhization and root meristem activity in the legume *Medicago truncatula*. *Plant J.* **2013**, *74*, 920–934. [PubMed]
52. Silva, G.F.F.E.; Silva, E.M.; da Silva Azevedo, M.; Guivin, M.A.C.; Ramiro, D.A.; Figueiredo, C.R.; Carrer, H.; Peres, L.E.P.; Nogueira, F.T.S. microRNA156-targeted SPL/SBP box transcription factors regulate tomato ovary and fruit development. *Plant J.* **2014**, *78*, 604–618.
53. García-Mauriño, S.M.; Rivero-Rodríguez, F.; Velázquez-Cruz, A.; Hernández-Vellisca, M.; Díaz-Quintana, A.; De la Rosa, M.A.; Díaz-Moreno, I. RNA binding protein regulation and cross-talk in the control of AU-rich mRNA fate. *Front. Mol. Biosci.* **2017**, *4*, 71.
54. Plass, M.; Rasmussen, S.H.; Krogh, A. Highly accessible AU-rich regions in 3′ untranslated regions are hotspots for binding of regulatory factors. *PLoS Comput. Biol.* **2017**, *13*, e1005460.
55. Curinha, A.; Oliveira, B.S.; Pereira-Castro, I.; Cruz, A.; Moreira, A. Implications of polyadenylation in health and disease. *Nucleus* **2014**, *5*, 508–519.
56. Li, W.; Zhang, Y.; Zhang, C.; Pei, X.; Wang, Z.; Jia, S. Presence of poly(A) and poly(A)-rich tails in a positive-strand RNA virus known to lack 3 poly(A) tails. *Virology* **2014**, *454–455*, 1–10.
57. Jing, Q.; Huang, S.; Guth, S.; Zarubin, T.; Motoyama, A.; Chen, J.; Di Padova, F.; Lin, S.C.; Gram, H.; Han, J. Involvement of microRNA in AU-rich element-mediated mRNA instability. *Cell* **2005**, *120*, 623–634. [PubMed]
58. Yang, L.; Xu, M.; Koo, Y.; He, J.; Poethig, R.S. Sugar promotes vegetative phase change in *Arabidopsis thaliana* by repressing the expression of MIR156A and MIR156C. *eLife* **2013**, *2*, e260.
59. Lee, J.H.; Lee, J.; Kim, H.; Chae, W.B.; Kim, S.J.; Lim, Y.P.; Oh, M.H. Brassinosteroids regulate glucosinolate biosynthesis in *Arabidopsis thaliana*. *Physiol. Plant.* **2018**, *163*, 450–458. [PubMed]
60. Liu, X.; Yang, Q.; Wang, Y.; Wang, L.; Fu, Y.; Wang, X. Brassinosteroids regulate pavement cell growth by mediating BIN2-induced microtubule stabilization. *J. Exp. Bot.* **2018**, *69*, 1037–1049. [PubMed]
61. Xia, K.; Ou, X.; Tang, H.; Wang, R.; Wu, P.; Jia, Y.; Wei, X.; Xu, X.; Kang, S.H.; Kim, S.K.; et al. Rice microRNA osa-miR1848 targets the obtusifoliol 14alpha-demethylase gene OsCYP51G3 and mediates the biosynthesis of phytosterols and brassinosteroids during development and in response to stress. *New Phytol.* **2015**, *208*, 790–802.
62. Kim, B.H.; Kwon, Y.; Lee, B.H.; Nam, K.H. Overexpression of miR172 suppresses the brassinosteroid signaling defects of bak1 in *Arabidopsis*. *Biochem. Biophys. Res. Commun.* **2014**, *447*, 479–484.
63. Feng, Y.; Kong, B.; Zhang, J.; Chen, X.; Yuan, J.; Tang, X.; Ma, C. Proteomic Analysis of vernalization responsive proteins in winter wheat Jing841. *Protein Pept. Lett.* **2018**, *25*, 260–274. [PubMed]
64. Kamarudin, A.N.; Lai, K.S.; Lamasudin, D.U.; Idris, A.S.; Balia, Y.Z. Enhancement of thiamine biosynthesis in oil palm seedlings by colonization of endophytic fungus hendersonia toruloidea. *Front. Plant Sci.* **2017**, *8*, 1799. [PubMed]
65. Copley, T.R.; Aliferis, K.A.; Kliebenstein, D.J.; Jabaji, S.H. An integrated RNAseq-(1)H NMR metabolomics approach to understand soybean primary metabolism regulation in response to Rhizoctonia foliar blight disease. *BMC Plant Biol.* **2017**, *17*, 84.
66. Wu, F.; Shu, J.; Jin, W. Identification and validation of miRNAs associated with the resistance of maize (*Zea mays* L.) to *Exserohilum turcicum*. *PLoS ONE* **2014**, *9*, e87251.
67. Dubouzet, J.G.; Matsuda, F.; Ishihara, A.; Miyagawa, H.; Wakasa, K. Production of indole alkaloids by metabolic engineering of the tryptophan pathway in rice. *Plant Biotechnol. J.* **2013**, *11*, 1103–1111. [PubMed]